



Modelling global solar radiation to optimise agricultural production

Agustín Domínguez-Álvarez, María-Teresa de-Tena-Rey and Lorenzo García-Moruno

University of Extremadura, Dept. of Graphical Expression, 06800 Mérida, Badajoz, Spain

Abstract

Aim of study: To present a complete global radiation model that includes direct, diffuse sky and ground-reflected radiation, and compare the values with those obtained by the pyranometers.

Area of study: The data were analyzed at the meteorological station network in Extremadura, Spain, to validate the results calculated by the model.

Material and methods: The method uses the maps from meteorological station data are based on a single piece of daily solar radiation data for an area of 8,000 to 9,000 ha, whereas the maps created by the models are obtained using the spatial resolution of the digital elevation model, in this case 25×25 m.

Main results: The analytical model used in the study obtained global radiation values with a difference of 1.44% relative to the values captured by the meteorological stations in Extremadura. Analysis of the data indicates that on days with a specific type of fog or very diffuse cloud, the global radiation captured by sensors is greater than it would be on clear-sky days in the same area. The method was suitable for calculating global solar radiation on any type of terrain with its corresponding diversity of crop types.

Research highlights: The research highlights the importance of understanding and modelling solar radiation for efficient use of water resources in agriculture. Adding these global radiation models to a GIS would provide a very valuable tool for developing regions.

Additional key words: solar radiation measurements; meteorology; remote sensing; solar energy.

Abbreviations used: DEM (digital elevation model); REDAREX (Irrigation Advisory Service, *Red de Asesoramiento al Regante de Extremadura*).

Authors' contributions: The three co-authors participated in all stages of the work, including the conception and design of the research, and the revision of the intellectual content. Funding acquisition, LGM. Methodology, project administration, and first draft of the paper, ADA. All authors read and approved the final manuscript

Citation: Domínguez-Álvarez, A; de-Tena-Rey, MT; García-Moruno, L (2021). Modelling global solar radiation to optimise agricultural production. Spanish Journal of Agricultural Research, Volume 19, Issue 1, e0201. <https://doi.org/10.5424/sjar/2021191-16813>

Received: 10 Apr 2021. **Accepted:** 04 Mar 2021.

Copyright © 2021 INIA. This is an open access article distributed under the terms of the Creative Commons Attribution 4.0 International (CC-by 4.0) License.

Funding agencies/institutions	Project / Grant
Government of Extremadura and the European Regional Development Fund (ERDF)	GR18176(to the research group “Diseño, Sostenibilidad y Valor Añadido INNOVA”)

Competing interests: The authors have declared that no competing interests exist.

Correspondence should be addressed to Agustín Domínguez-Álvarez: adomguez@unex.es

Introduction

Efficient and proper use of water resources in agriculture is one of the main challenges in recent times. Developed countries therefore study the agrometeorological parameters associated with agricultural water resource management in their territory. In many aspects of environment and engineering sciences it is important to have accurate knowledge of solar radiation and its characterisation on the Earth's surface (Kaskaoutis & Polo, 2019). The high spatial and temporal variability of Earth's solar radiation is the result of the radiative transfer that occurs in the atmosphere. The importance of this variability in

climate studies has led to considerable efforts to improve the capabilities of modelling to determine the components of solar radiation (Polo *et al.*, 2019).

The energy that the sun supplies to Earth in the form of electromagnetic radiation is used in photosynthetic processes, surface and atmospheric heating, evaporation and transpiration. Climate, in turn, is determined by the effect of solar energy on atmospheric heating and evaporation, indicating the importance of sky conditions on crop yields (Changnon & Changnon, 2005; Pandey & Kariyar, 2013). The amount of incident solar radiation in a region is determined by astronomical, geographical and topographical factors, and influenced by other

factors such as atmospheric transparency and sunlight, the topography of the terrain, the atmospheric water vapour content, the elevation of the sun and the duration of the day. Solar radiation is the principle factor in determining the microclimate of a crop. Its energy conditions air and land temperature, wind movement, evapotranspiration and photosynthesis. The intensity of the radiation, the degree of interception, and efficient use of radiant energy are determining factors in plant growth rates (Sandaña *et al.*, 2012).

Solar radiation and its fluxes are highly variable in time, space, climate, season and other factors (Solanki, 2002). The spatial distribution of organisms and plants responds to solar radiation fluxes. In agriculture, plants are living beings that transform solar energy, making it available to humans and animals. Solar radiation directly affects crops through photosynthesis, but it also affects soil and plant evaporation through temperature, which in turn affects soil water balance (an agrometeorological factor) (Ferrante & Mariani, 2018).

To optimise the use of solar energy, an in-depth study is needed of the solar radiation components received by the Earth's surface. However, the information available in most works is outdated or incomplete. Interpolating surface solar radiation obtained from surface meteorological stations does not permit analysis of micro-climate aspects of solar irradiation (Zelenka *et al.*, 1999; Muneer *et al.*, 2007; Kambezidis, 2016). This illustrates the importance of detailed estimation of solar radiation over the whole terrestrial surface.

According to the standard atmosphere model (Mitjá & Batalla, 1982), the estimate of the global irradiance (W/m^2) incident on the Earth's surface may be divided into direct, diffuse and ground-reflected radiation:

$$E_t = E_i + E_d + E_r,$$

where: E_t , total irradiance; E_i , direct solar irradiance; E_d , diffuse sky irradiance; E_r , ground-reflected irradiance.

To estimate the irradiance incident on the Earth's surface (Fig. 1), we need to know, firstly, the solar irradiance that reaches beyond the Earth's atmosphere. This value is known as exo-atmospheric solar irradiance or solar constant (S_0). The mean value of the solar constant determined by the WMO (1982) is $1367 W/m^2$. The value of the solar constant is obtained using the mean distance between the Earth and the sun in its annual orbit.

In the last 20 years, the number of automatic meteorological station networks has increased considerably around the world. This rapid development was due to the need for meteorological data in near-real time and significant advances in automatic data acquisition systems. The Irrigation Information Service (SIAR) is Spain's largest automatic meteorological network. Installed in 1999-2000, it covers most irrigation areas in Spain and was

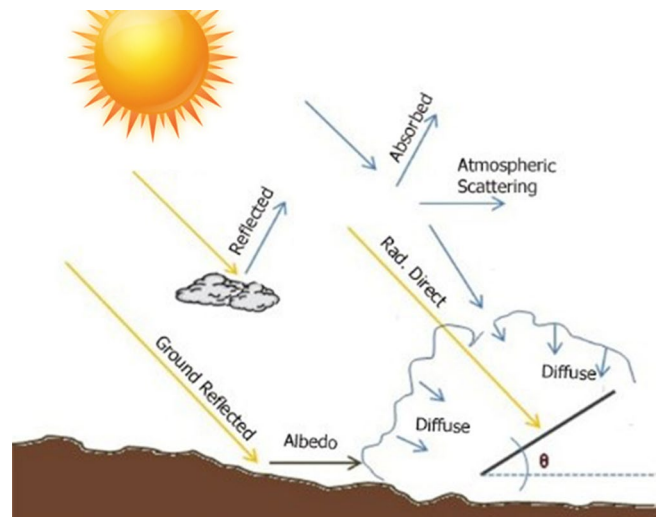


Figure 1. Solar radiation components. *Source:* Authors' own figure.

established across the country for agronomic purposes (Estévez *et al.*, 2011).

Spatialising meteorological data is a very difficult task, especially in heterogeneous terrain. For some time, particular emphasis has been placed on developing spatialisation methods (Bindi & Gozzini, 1998; Gozzini & Homs, 1998) and comparing interpolation methods (Gozzini & Paniagua, 2000; Gattioni *et al.*, 2011). Numerical weather prediction methods are now the main tools that scientists use to study the behaviour of meteorological events and propose explanations about their formation and development (Xue & Fennessy, 1996; Lynch, 2008).

Many research centres and universities around the world have a forecasting service based on the results of numerical models, in particular the Weather Research and Forecasting model (WRF). The WRF is a next-generation mesoscale model developed by United States institutions, including the National Center for Atmospheric Research (NCAR), National Center for Environmental Prediction (NCEP) and Forecast Systems Laboratory (FSL). It was designed for use in both operational forecasting and atmospheric science research (Michalakes *et al.*, 2004).

This study on modelling global solar radiation for any location on the Earth's surface that has a digital elevation model (DEM) is important because the methodology is the only viable option for developing countries with no meteorological station network. The model was tested with data obtained in the field by pyranometers (Fig. 2) in the Extremadura region meteorological station network. The network website, Agralia, belonging to the Irrigation Service of the Directorate General of Rural Development (Extremadura Regional Government), provides advice, monitoring and support for irrigators through the Irrigation Advisory Service (REDAREX), informing them about crop water needs and enabling them to programme irrigation efficiently according to specific requirements



Figure 2. SKYE SP1100 or CM3 pyranometers. *Source:* REDAREX (Extremadura Regional Government).

and climate and soil conditions. All that is needed for this estimation is a geographical reference.

Because it is important to calculate solar radiation using all of its components, the novelty of this study is that it includes analytical calculation of ground-reflected radiation (E_r).

Material and methods

Study area

The study area is in the region of Extremadura, in the southwest of the Iberian Peninsula, and comprises the two largest provinces in Spain (Fig. 3): Cáceres and Badajoz. Our pilot work area in Extremadura is the area identified in Sheet_575_Hervás MAGNA50, georeferenced with a latitude of $40^{\circ}20'4.41''N$ and longitude of $6^{\circ}11'39.51''W$, in the province of Cáceres, part of the Ambroz Irrigation Area.

The characteristics of the relief in Extremadura give rise to a climate that is subject to numerous influences. The solar radiation received is the highest in mainland Spain. At midday, Cáceres and Madrid (continental Mediterranean climate) have similar values of around 750 W/m^2 , followed by Murcia (east coast) with values of about 650 W/m^2 and Santander (north coast) with values of about 500 W/m^2 (Pérez-Burgos *et al.*, 2014).

Because the main objective of meteorological networks is to determine crop water needs, the meteorological stations in Extremadura are located in irrigation areas, with an equipment density of one station every 8,000-10,000 ha to characterise the climate of the areas.

Each station occupies a horizontal area of $10 \times 10\text{m}$ sown with the reference crop, in this case grasses, irrigated by sprinkler irrigation. All stations are connected by digital GSM to the Irrigation Management Centre, in Mérida, and the server at the Extremadura Research and

Technological Development Service at La Orden-Valdesquera Research Centre, in Guadajira (Badajoz).

Material used

Digital cartography

The study was conducted using official maps from the National Geographical Institute, available at the Extremadura Regional Government Department of Agriculture, Rural Development, Environment and Energy, and the algorithms necessary to model solar radiation (Dominguez, 2015). The DEM of the terrain has a $25 \times 25\text{m}$ grid size, with official sheet distribution of 1:25000, ETRS89 geodetic reference and UTM Projection in the corresponding time zone. The DEMs of the study area (region of Extremadura) were obtained, and in particular of the province of Cáceres, because it has more pronounced orography and would have more impact in the calculation of reflected radiation. The final solar radiation calculation can be used anywhere in the world that has a DEM available.

Historical meteorological data

From the historical agrometeorological data (Table 1) provided on the REDAREX website, we chose only the data relevant for the study: solar radiation (MJ/m^2) and insolation hours. The early date chosen, 1 July 2012, rather than a date closer to the present, was conditioned by the search for days with least possible cloud cover, as shown in the daily 'insolation hours' column. This date was the best match for the selection criterion.

Methods

A further objective of this work was to validate the direct and diffuse radiation models presented. This allows us to calculate ground-reflected radiation as a factor to include in future studies on improving topographic correction models for the classification of multispectral satellite images (Hantson & Chuvieco, 2011; Zhu *et al.*, 2017; Xiao *et al.*, 2018).

The direct component from the sun is directional and therefore its influence depends on the location of the sun and the slope and orientation of the exposed location. The diffuse component comes from atmospheric diffusion and dispersion (scattering), and is normally considered a hemispherical light source (omnidirectional). The reflected component comes from the surrounding terrain and therefore depends on the spatial location of a place and its topographical environment.

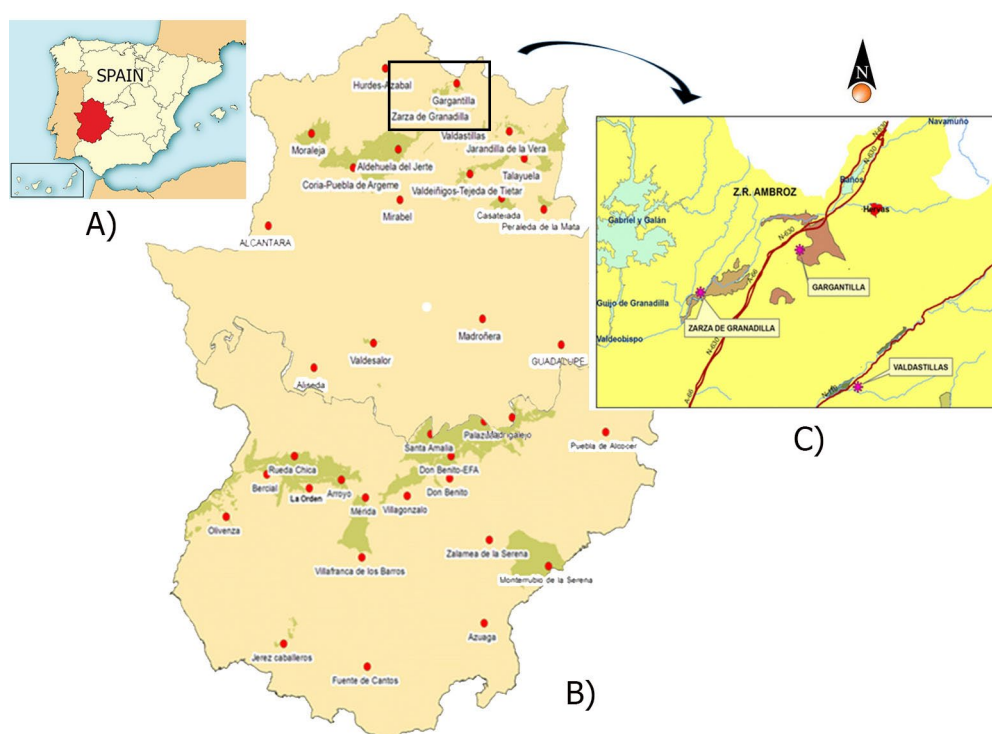


Figure 3. Study area: (A) Extremadura, Spain; (B) Meteorological station network; (C) Ambroz Irrigation Area, Cáceres. *Source:* REDAREX (Extremadura Regional Government).

Algorithms of direct solar radiation (R_{direct}) and diffuse sky radiation ($R_{diffuse}$)

Previous studies reported that short-wave solar radiation from a clear sky varies in response to altitude and elevation, surface gradient (slope) and orientation (aspect), as well as position relative to neighbouring surfaces (Zimmermann, 2000a,b; Corripio, 2002). Kumar used a DEM to calculate possible direct solar radiation and diffuse radiation over a large area. This model was used as a reference to create our own algorithms using a different programming language.

The R_{direct} algorithm (Domínguez, 2015) (Fig. 4) was created by taking into account the areas of topographic shading resulting from the DEM used. In these shaded areas in which no direct radiation is received, diffuse and reflected radiation have a more relevant role because they are the only types of radiation received and

therefore it is important to estimate them in these types of locations.

The $R_{diffuse}$ algorithm (Domínguez, 2015) (Fig. 4) was developed to suit the climate regime of the area, for clear-sky days, and therefore without taking into account the reduction of solar radiation due to cloud cover.

The following data were needed to develop the R_{direct} and $R_{diffuse}$ algorithms: DEM; sun trajectories for the day, month and year; earth-sun distances; incidence angle at each point of the DEM; topographic shading model.

Algorithms of ground-reflected radiation ($R_{G.reflected}$)

The $R_{G.reflected}$ algorithm (Domínguez, 2015) (Fig. 5) was created using the data obtained from the direct

Table 1. Agrometeorological data obtained from the meteorological stations Guadajira-La Orden (Badajoz), from 01 Jul 2012 to 04 Apr 2012. *Source:* REDAREX.

Max temp (°C)	Min temp (°C)	Max hrs (%)	Min hrs (%)	Solar rad. (MJ/m ² day)	Net rad. (MJ/m ² day)	Mean wind speed (m/s)	Max wind speed (m/s)	Wind direction (°)	ETo (mm)	Insolation hours
28.8	11.7	79	12.3	31.4	16.2	2.1	6.6	265	6.8	13.5
33.1	11.2	82.4	10.1	30	15.5	1.3	4.8	252	6.3	13.3
33.5	14.1	79	21.2	29.4	16	2.3	6	296	7.4	13.4
30.1	15.8	84.9	29	30.6	17.1	3.6	7.4	300	7.5	13.5

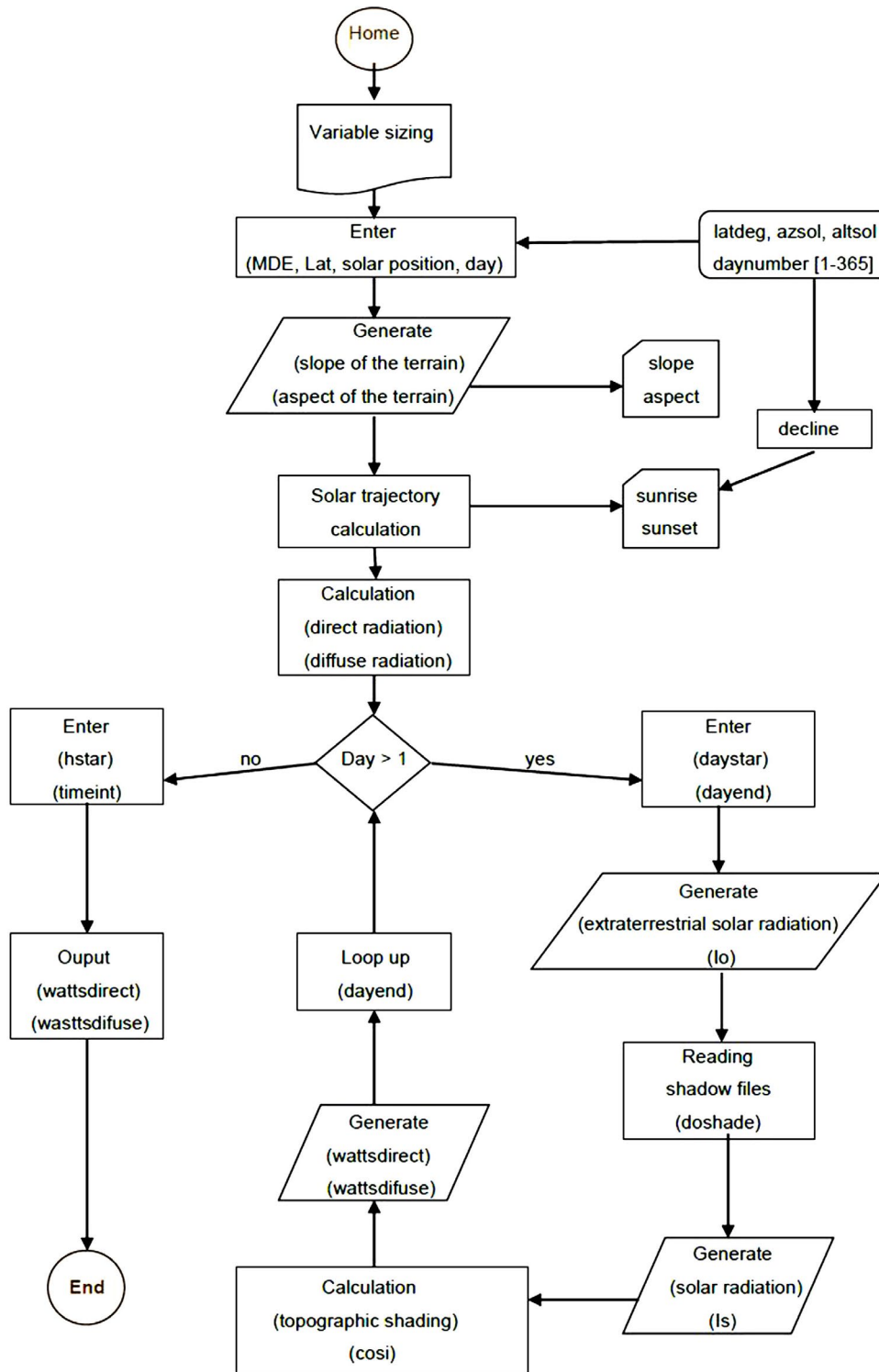


Figure 4. Flowchart of calculation of direct and diffuse solar radiation. Authors' own figure.

and diffuse radiation, taking into consideration the loss of light intensity by the inverse of the square of the distance.

The direction of a vector in space is calculated using the direction cosines ($\cos \alpha$, $\cos \beta$, $\cos \gamma$) relative to the X, Y and Z axes.

In our case, the calculation of the angle between two surfaces is the same as the calculation of the angle between

the normals to these surfaces, and the effect is similar to the reduction of the solid angle of a surface with an inclination relative to the direction of light and a specific distance.

To model this reduction due to the angle between two surfaces (Fig. 6a), we performed the following reductions:

- Calculation of cosine alpha (Top view of Fig. 6b): this is the reduction that occurs due to the inclination of

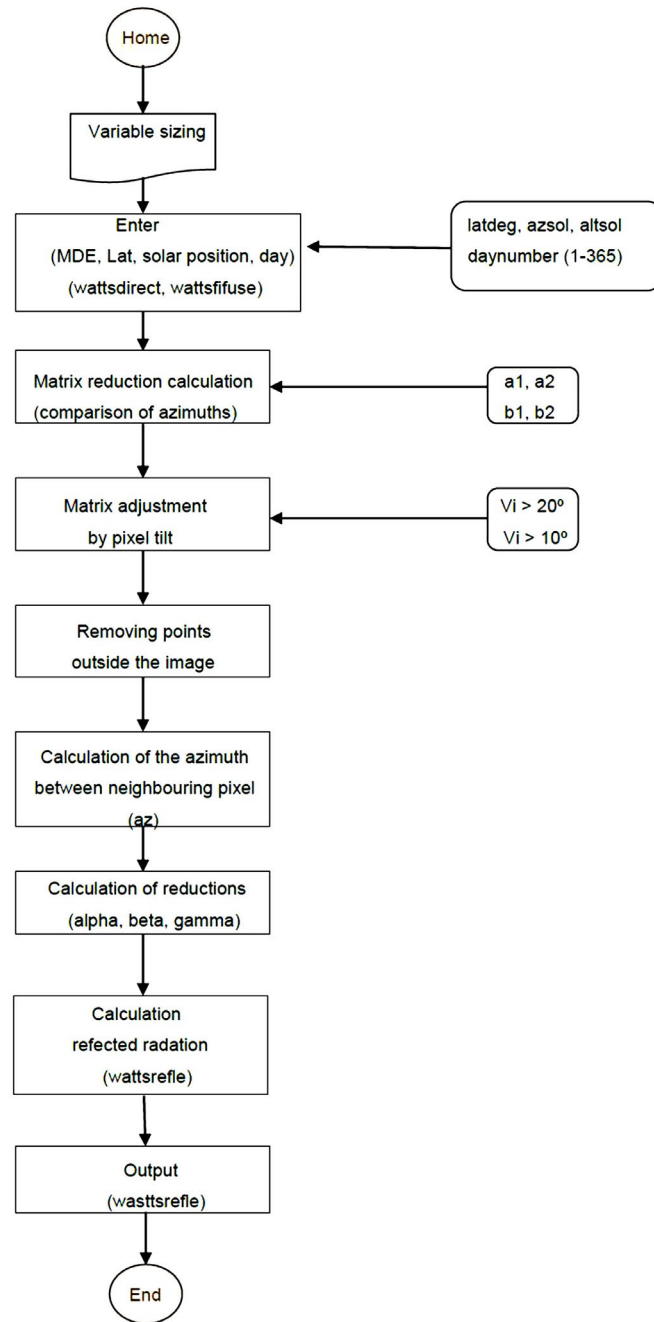


Figure 5. Flowchart of calculation of ground-reflected solar radiation. Authors' own figure.

the refracting surface relative to the azimuthal angle between the refracting surface and the problem surface. This angle is obtained using the following formula:

$$\alpha = \text{abs}(AZ + 180 - af)$$

where alpha is the absolute value between the difference of the azimuthal angle of the two surfaces (AZ) and of the azimuthal angle of the reflecting surface (af). Alpha cosine is maximum (1) when the reflecting surface is perpendicular to the direction between the two surfaces (alpha=0) and minimum (0) when the surface is in

profile relative to the direction between the two surfaces (alpha≥90).

– Calculation of cosine beta (Front view of Fig. 6b): this is the reduction that occurs due to the angular difference between the reflecting surface and the normal relative to the problem surface. This angle is obtained using the following formula:

$$\beta = \text{abs}(AZ - ai)$$

where beta is the absolute value between the difference of the azimuthal angle of the two surfaces (AZ) and of

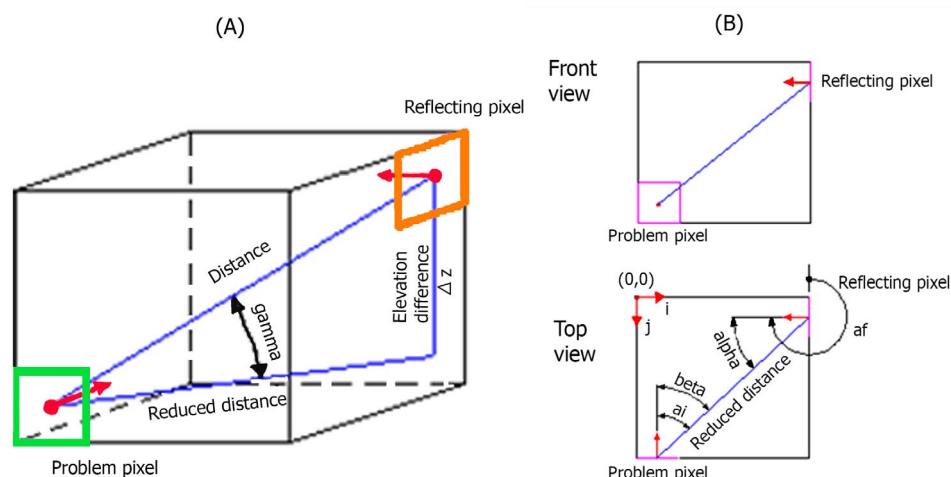


Figure 6. Spatial position between problem surfaces (A); front and top views (B). Authors' own figure.

the normal relative to the problem surface (a_i). Cosine beta is maximum (1) when the angle between the reflecting surface and the normal surface of the problem surface is zero ($\beta=0$) and minimum (0) when this angle is greater than or equal to 90 ($\beta \geq 90$).

- Calculation of gamma cosine (Fig. 6a): this is the reduction that occurs due to the difference in elevation between the two surfaces; it is the vertical angle between the reflecting surface and the problem surface. The value of this angle is the arctangent between the difference in elevation (Δz) of the two surfaces and the distance between the two surfaces:

$$\text{gamma} = \arctg \left(\frac{\Delta z}{\text{Distance}} \right)$$

where gamma cosine is maximum (1) when the difference in elevation is zero and minimum (tends to 0) when the difference in elevation tends to infinity.

The total reduction between the problem surface and all the surrounding surfaces is the product of these three direction cosines; alpha cosine, beta cosine and gamma cosine.

Model testing

The models were verified and compared with the data collected from the REDAREX meteorological stations. The stations are on horizontally level terrain, a circumstance that had to be included in the algorithms. Readings of global solar radiation incident on a horizontal surface are necessary for various applications in fields such as agriculture, architecture, hydrology, solar collector engineering and meteorology. However, for some of these applications, radiation must be divided into direct and diffuse components.

Solar radiation maps

Global solar radiation maps were generated, modelled by the algorithms and also developed from the meteorological station data, and the two types of maps were compared.

Statistical analysis

To conduct a statistical check between the solar radiation values “Observed” in the field at the meteorological stations and the values “Modelled” with the algorithms, we performed a t-test, or Student’s t-test, the statistical test that is best suited to this type of analysis.

A t-test is any test in which the statistic used has a Student’s t distribution if the null hypothesis is true. It is used when the population studied follows a normal distribution but the sample size is too small for the statistic on which the inference is based to have a normal distribution, and therefore an estimate of the standard deviation is used instead of the real value. It is applied in discriminant analysis (Table 2):

T-TEST: COMPUTE Differences=Observed-Modelled.

/TESTVAL=0 /MISSING=ANALYSIS /VARIABLES=Differences /CRITERIA=CI(.95) /MAE=0.70 /RMSE=0.917

where MAE is the mean absolute error, RMSE is the root mean square error, where the mean of -0.197 is below the recording range of the meteorological stations and the standard deviation of 0.907 is not large even though the sample is not large either.

It is important to note that because the “asymptotic significance (bilateral)” statistic is a value that is not close

Table 2. Statistics: (A) Statistics for a sample in the T-test; (B) T-test for the differences sample; (C) Ranges of the differences sample in the t-test.

A)	N	Mean	Std. deviation	Typical error of the mean
	37	-0.1974	0.90760	0.14921
Test value = 0				
B)	t	df	Sig. (bilateral)	Difference of means
	-1.323	36	0.194	-0.19736
Test value = 0				
95% confidence interval for the difference				
C)	Lower		Upper	
	-0.5000		0.1052	

to 0.05, this test indicates that the relation between the Observed and the Modelled data is very good.

The range of values (Lower and Upper) for a 95% confidence interval for the value of the difference includes the value 0 (value indicating a perfect match between Observed and Modelled values). Because the Lower and Upper ranges include the value 0, there is no discrepancy of either undervaluation or overvaluation of the values modelled by the algorithms.

Results

Application of the proposed method

The algorithms were computer programmed using IDL programming language, run, and checked using theoretical testing models (Domínguez, 2015). The working area (Hervás) was chosen because of its pronounced orography. The date chosen from the wide range available through REDAREX was 1 July 2012, because it was the day with least cloud cover (clear-sky day).

Gradient models

Using the matrices of azimuth and solar elevation for the time interval chosen between sunrise and sunset obtained with the programme ENVI, models were calculated for azimuthal orientation (aspect) and gradient (slope), from worksheet 575, using the DEM of the area (Fig. 7).

The models of shade in the area (Fig. 8) were then calculated for each time interval chosen (5.00 to 19.00 hours), showing the areas with topographic shading during the day.

Direct solar radiation model (*Rad.direct*)

The direct solar radiation model (Fig. 9a) was generated through the programme ENVI using the two gra-

dient models for the day and the area chosen. All the radiation models calculated by the algorithms and viewed by the programme are numerical ASCII files, with the solar radiation values for each pixel of the terrain given in MJ/m².

The image shows that the maximum radiation on the Earth's surface is obtained on surfaces that are more orthogonal to the direction of light rays, coinciding with the hours of solar midday. Surfaces at more than 90° relative to the solar direction appear as shading, with considerably less direct solar radiation or even no radiation in some areas.

In some cases, the orography of the mountainous terrain prevents visibility of the sun, causing topographic shading and therefore less direct solar radiation in these areas (north-facing slopes).

Diffuse sky radiation model (*Rad.diffuse*)

The R.diffuse algorithm was executed using the elevation model, illustrating how this radiation depends on the altitude of the location. The diffuse radiation model (Fig. 9b) had higher radiation in areas with thinner atmospheric mass (areas at higher altitude) and less radiation at lower altitudes.

Ground-reflected radiation model (*R.G.reflected*)

The R.G.reflected algorithm was executed using the radiation models and the two gradient models, stopping at 1500 m, because after this distance the intensity of the radiation is greatly reduced by the inverse of the square of the distance.

The ground-reflected radiation obtained (Fig. 9c) indicates that this type of radiation is not detected in locations that are practically horizontal (as expected), although maximum reflected radiation is obtained in areas close to the abrupt change of two slopes with opposing faces, such as watercourses, and in low areas of mountain slopes.

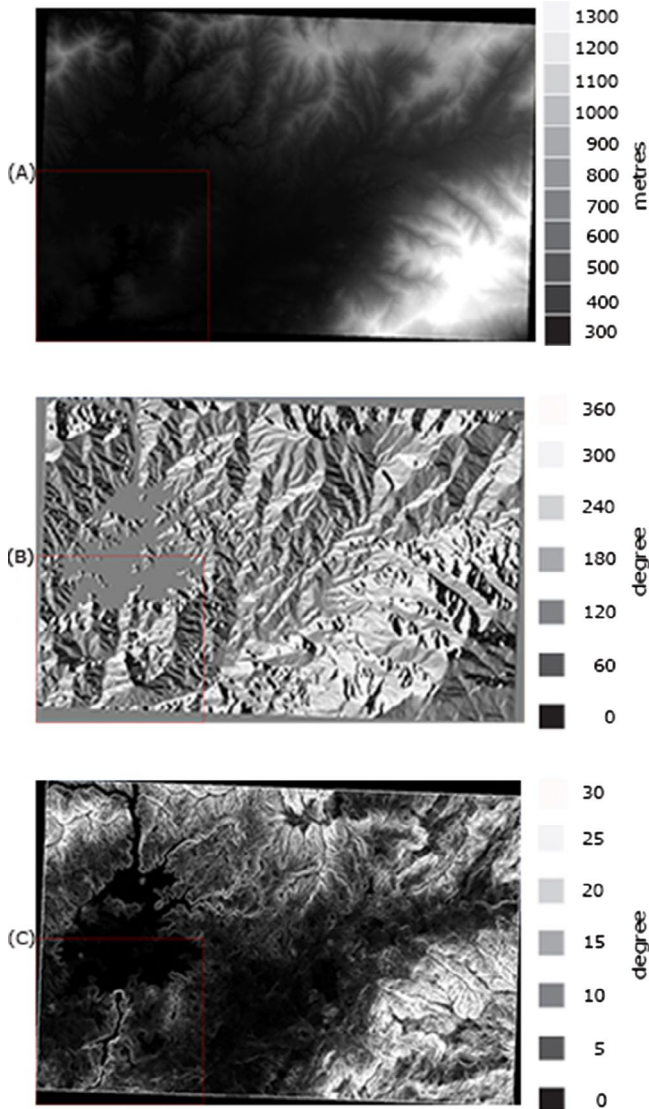


Figure 7. Digital elevation model (A); aspect model (B); and slope model (C). Sheet_575. Envi.

Map of global solar radiation modelled by the algorithms (Rad.global)

The sum of the matrices of the three models (Rad.direct, Rad.diffuse and Rad.G.reflected) corresponds to the following global radiation model (Fig. 9d).

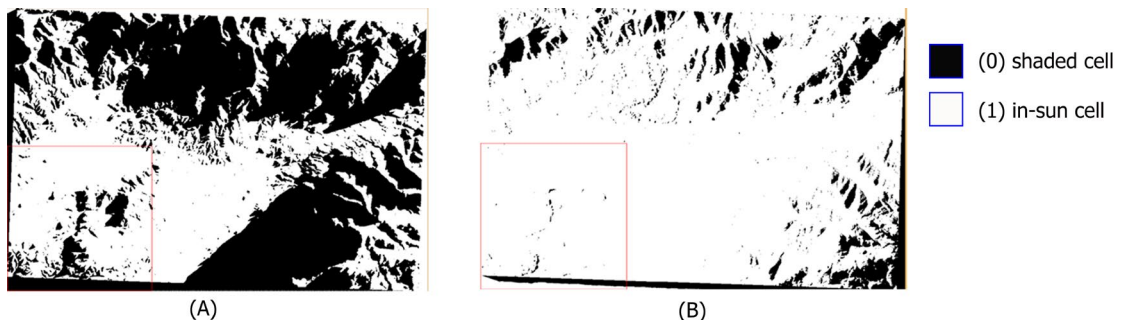


Figure 8. Examples of shading models: (A) sunrise (5.00 h); (B) sunset (18.00 h). Envi.

The Rad.global model is a numerical ASCII file with the solar radiation values for each pixel of the terrain given in MJ/m², represented as an image in which lighter tones indicate higher global radiation and darker tones indicate lower global radiation.

Using the global radiation model obtained with the algorithms, we can perform an unsupervised classification (ISODATA) for a visual reference of the classes calculated automatically by the programme according to the distribution of the data. This initial classification breaks the data down into seven categories of solar radiation, from practically zero values due to topographic shading to values higher than 32.5 MJ/m² in areas more receptive to the direction of the sun. With these classes calculated automatically, a supervised classification (minimum distance) was performed (Fig. 10), creating digital seals (ROIs) that were best adapted to the area in question, given that a large part of it is under water because of the Gabriel y Galán dam, which must be shown, differentiated and not included with other classes of terrain.

REDAREX global solar radiation map

On the website created by REDAREX, the Extremadura irrigation service, we can identify the geographical location of the stations closest to the irrigation site and calculate the mean solar radiation from the values recorded at the stations (Fig. 11). These are standard meteorological stations, on a horizontal area of 10 × 10 m, located every 8,000 to 10,000 ha.

These data therefore do not take into account the characteristics of gradient or topographic shading in other irrigation areas around each station.

Comparison of observed and modelled data

Global radiation values calculated with algorithms

Table 3 shows the data generated by the algorithms of direct radiation and diffuse radiation from each horizontal

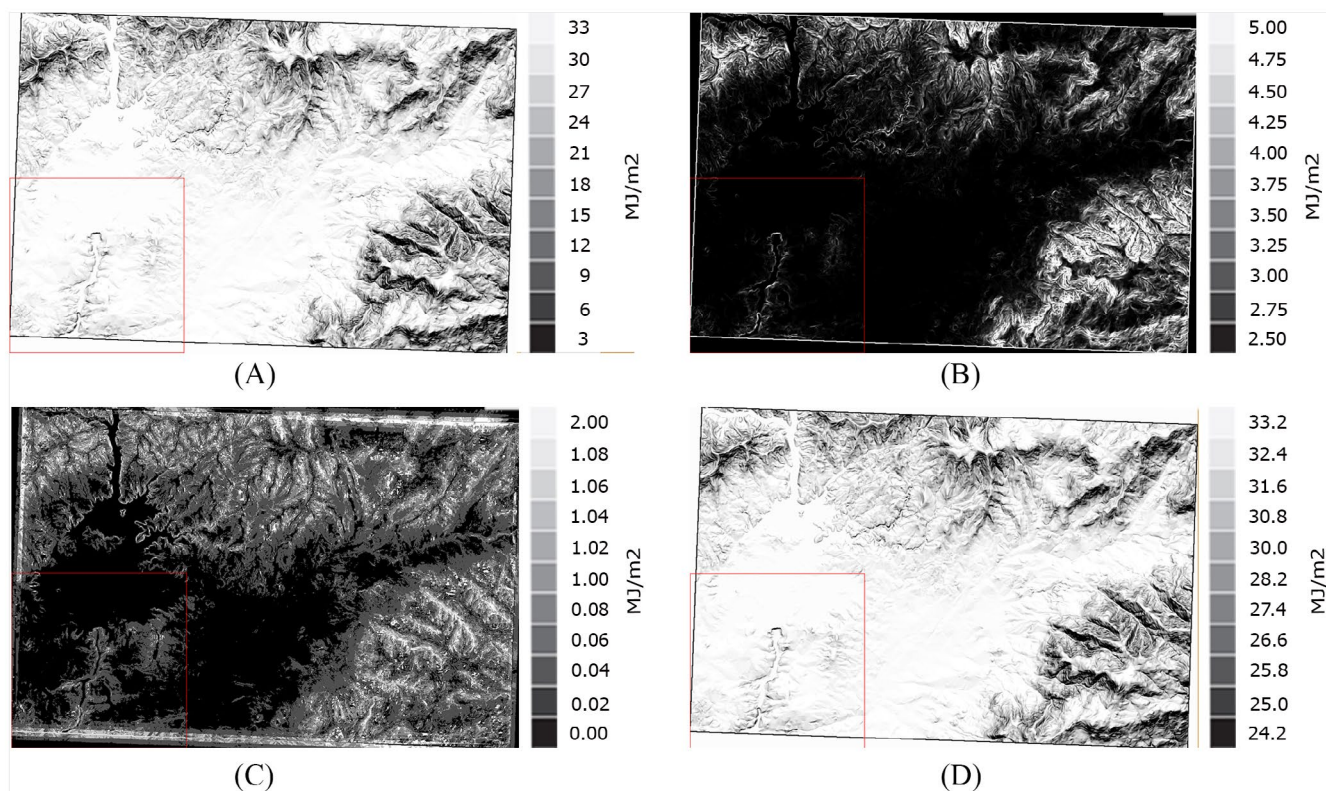


Figure 9. Solar radiation: Direct solar radiation model (A); diffuse sky radiation model (B); ground-reflected radiation model (C); and global radiation (D). Envi.

theoretical model corresponding to the locations of the meteorological stations.

Solar radiation values obtained by the Agrometeorological Station Network.

To ensure that the solar radiation data collected were as similar as possible to the model data, the historical data (Table 1) for the days with minimum cloud cover were obtained, corresponding to the days with most hours of solar radiation, shown in the column 'Insolation Hours'. Table 1 shows the solar radiation values from all the stations for the chosen date.

Comparison of methods

After obtaining the solar radiation data recorded at the meteorological stations in the region and the data estimated by the computer algorithms, the data were compared, taking the following circumstance into account:

Officials at the REDAREX have observed that on some days with a certain level of cloud cover, the pyranometers capture more solar radiation than they would if the sky were clear, due to a possible atmospheric rebound effect, where the highest solar radiation intensity

is detected not when the sky is clear, but when it is partly clouded by convective clouds (Matuszko, 2012). In addition, broken bright clouds near the sun's disk may significantly increase the diffuse irradiance measured (Psiloglou *et al.*, 2019).

Bearing this circumstance in mind, we analysed the difference obtained in the capture of global solar radiation by the two methods, shown in Fig. 12.

Table 3 shows how the effect of fog is produced in the capture of solar radiation by the meteorological station pyranometers. Although it is minimal in most cases, at the Zarza de Granadilla and Madroñera stations (both in the province of Cáceres) there is a difference of 3.69% and 5.87%, respectively, relative to the data calculated analytically on what was considered a clear-sky day.

The mean difference observed between the data obtained by the two methods is 1.44% of total global radiation, much less than initially expected. The mean difference was 1.71% in the province of Badajoz and 1.18% in the province of Cáceres.

The histogram (Fig. 13) corresponding to the t-test of the Differences statistic, which indicates the value of the mean, standard deviation and sample number, shows that the frequency distribution is centred around values close to 0. The closer the values are to 0, the better the Modelled values will be relative to the Observed values.

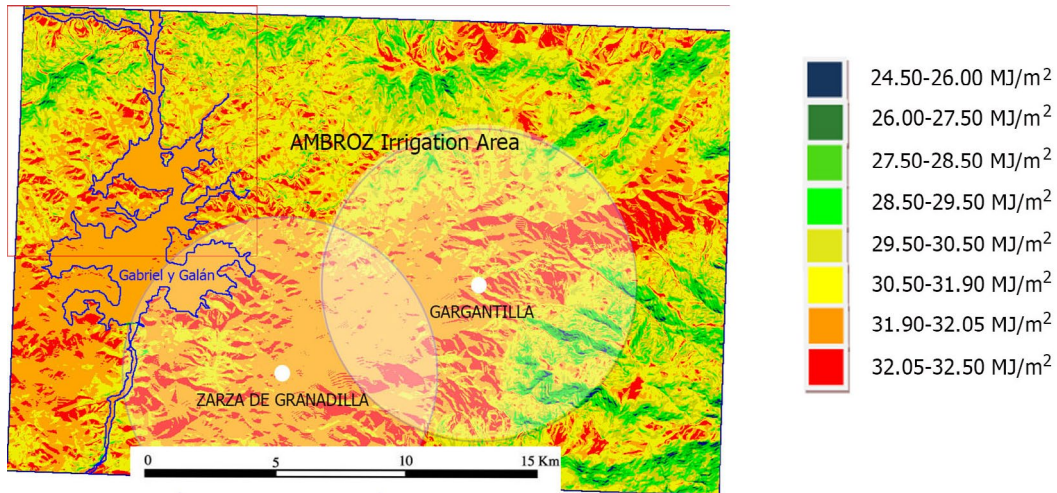


Figure 10. Supervised classification by minimum distance of the solar radiation modelled.

Discussion

This research study addresses the analytical calculation of global solar radiation models and their considerable potential in various applications of remote sensing, especially in classifying images for agricultural use. The results pave the way for new initiatives to continue and extend this line of research and the possibility of examining novel lines of complementary research.

As shown, the analytical models proposed for the calculation of direct, diffuse and reflected radiation provide the results of estimating global solar terrestrial radiation for any location on Earth that has a DEM available. This estimate can be made for any hour of the chosen day, month or year, whether it is in the past (useful for checking the proposed models), the present (for real daily studies) or the future (short- and med-term forecasting for sowing the most suitable plant varieties for the global radiation forecast).

When the direct and diffuse solar radiation results obtained in this study were compared with the results obtained by Zimmermann (2000a,b) using algorithms created with a different AML programming language (ARC/INFO Macro Language), it was found that the results were the same.

The analytical models used in the study obtained global radiation values with a difference of 1.44% relative to the values captured by the meteorological stations in Extremadura. The percentage is very low, despite all the technical implications in both the configuration of the models and the equipment used at the meteorological stations. The difference is the mean of the values obtained in the two provinces of Extremadura (1.71% difference in Badajoz and 1.18% in Cáceres). This indicates that the modelled data are more similar to the data obtained by the meteorological stations in areas with less relief than in mountain areas. Some climate factors are difficult to predict, such as days with a certain type of fog or very diffuse cloud cover, because in these cases the global

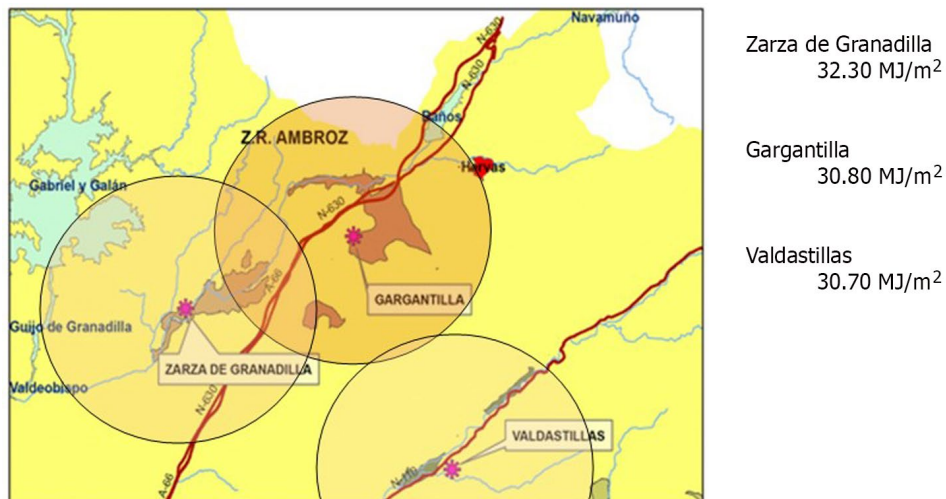


Figure 11. REDAREX solar radiation map: La Zarza de Granadilla, Gargantilla and Valdastillas

Table 3. Difference (%) in global radiation between methods.

Stations	Radiation from algorithms (MJ/m ²)			Radiation from meteorological stations (MJ/m ²)			Difference (%)
	Direct	Diffuse	Global	Latitude N	Altitude (m)	Global	
Badajoz							
Olivenza	28.59	2.52	31.11	38.4320	202	30.03	3.60
Talavera la Real–Berc.	28.58	2.53	31.11	38.5300	200	30.77	1.10
Pueblonuevo-RdaChic	28.58	2.53	31.11	38.5500	186	30.21	2.98
Guadajira – La Orden	28.58	2.53	31.11	38.5100	186	31.35	-0.77
Jerez de los Caballeros	28.59	2.52	31.11	38.1658	261	30.31	2.64
Arroyo de San Serván	28.58	2.53	31.11	38.5200	220	31.72	-1.92
Mérida	28.58	2.53	31.11	38.5047	265	31.17	-0.19
Villafranca los Barros	28.59	2.52	31.11	38.3406	406	31.10	0.03
Fuente de Cantos	28.60	2.52	31.12	38.1235	600	31.61	-1.55
Santa Amalia	28.56	2.53	31.09	39.0053	248	31.03	0.19
Villagonzalo	28.58	2.53	31.11	38.5017	266	31.03	0.26
Don Benito - EFA	28.58	2.53	31.11	38.5800	260	31.89	-2.45
Don Benito	28.58	2.53	31.11	38.5443	267	30.88	0.74
Palazuelo	28.56	2.53	31.09	39.0600	290	30.24	2.81
Zalamea de la Serena	28.59	2.52	31.11	38.4048	459	32.04	-2.90
Azuaga	28.59	2.52	31.11	38.2333	540	32.24	-3.50
Monterrubio la Serena	28.59	2.52	31.11	38.3535	499	31.25	-0.45
Puebla de Alcocer	28.56	2.53	31.09	39.0433	500	30.25	2.78
Cáceres							
Alcántara	28.54	2.54	31.08	39.4452	327	31.61	-1.68
Coria–PueblaArgeme	28.54	2.54	31.08	40.0259	252	29.21	6.33
Aliseda	28.56	2.54	31.10	39.1634	327	31.53	-1.36
Moraleja	28.51	2.55	31.06	39.5816	235	28.64	8.52
Hurdes - Azabal	28.51	2.56	31.07	40.1800	574	31.25	-0.58
Aldehuela del Jerte	28.52	2.55	31.07	40.0034	262	30.36	2.34
Valdesalor	28.55	2.54	31.09	39.2206	382	31.48	-1.24
Mirabel	28.54	2.54	31.08	39.5116	541	31.13	-0.16
Zarza de Granadilla	28.52	2.55	31.07	40.1259	380	32.26	-3.69
Gargantilla	28.51	2.56	31.07	40.1428	596	30.76	1.01
Valdastillas	28.51	2.55	31.06	40.0757	634	30.73	1.07
Tejada de Tiétar	28.54	2.54	31.08	39.5738	235	29.52	5.28
Madroñera	28.55	2.54	31.09	39.2758	625	33.03	-5.87
Jarandilla de la Vera	28.51	2.55	31.06	40.0608	508	30.24	2.71
Talayuela	28.52	2.55	31.07	40.0047	277	29.37	5.79
Madrigalejo	28.56	2.53	31.09	39.0813	297	30.35	2.44
Peraleda de la Mata	28.54	2.54	31.08	39.5136	309	31.29	-0.67
Guadalupe	28.55	2.54	31.09	39.2318	740	30.88	0.68
Casatejada	28.54	2.54	31.08	39.5209	274	30.64	1.44

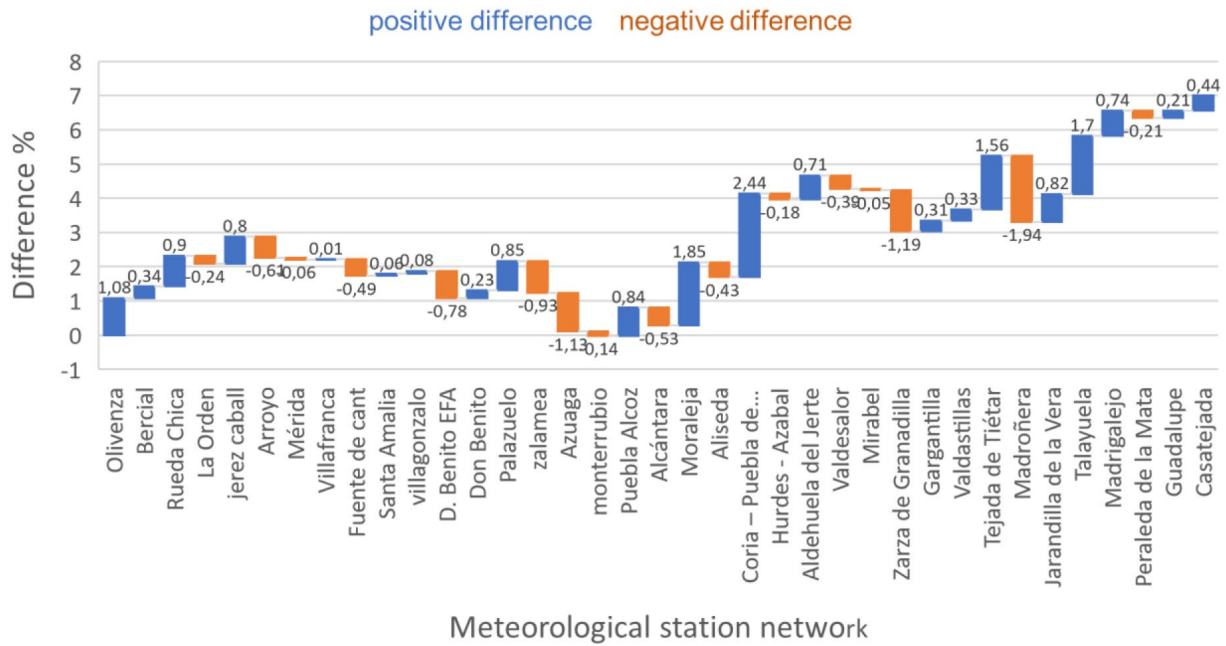


Figure 12. Difference in global radiation between methods.

radiation captured by the sensors is higher than it would be on clear-sky days in the same area. This circumstance has been tested and corroborated by officials from the Irrigation Service, who made their radiometers available for testing and informed us that this effect usually occurs in areas of the province of Cáceres, perhaps due to the climate characteristics and more pronounced relief than in the province of Badajoz.

The global solar radiation data provided by the Extremadura agrometeorological stations are obtained at each station installed approximately every 9,000 ha in a horizontal area. However, the models for this study generate a thematic map with individual global radiation values of the terrain for every 25 × 25 m spatial resolution of the

map, also taking into account the gradient of the terrain and the topographic shading caused by the orography. Given the considerable advantage of this tool and methodology, they can be used to calculate global solar radiation not only for extensive irrigation areas that typically have a flat or gentle relief, but also for mountain areas with pronounced relief where terrestrial solar radiation is highly variable because of the gradient and topographic shading, where other plant species are grown in accordance with the global radiation received.

Running these global radiation models in a GIS would be a very valuable tool for developing regions, because no large investment is needed to parametrise the agrometeorological information and the only requirements are a computer and easily obtainable DEMs of the terrain.

This study presents a tool for calculating global solar radiation for any geographical area that has a DEM available. The data were compared with the data captured by meteorological stations and had a mean accuracy value of 1.44%. The data show that global radiation can be calculated analytically using the proposed algorithms. Analysis of the data indicates that on days with a specific type of fog or very diffuse cloud, the global radiation captured by sensors is greater than it would be on clear-sky days in the same area. Further research is necessary to disentangle the factors that influence and generate this atmospheric phenomenon and analyse them in greater depth.

As described above, the method is suitable for calculating global solar radiation on any type of terrain with its corresponding diversity of crop types. Adding these global radiation models to a GIS would provide a very valuable tool for developing regions.

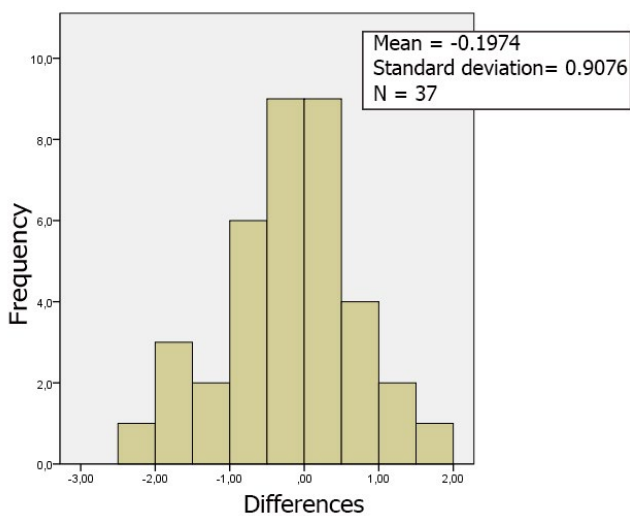


Figure 13. Histogram of the differences variable. Source: SPSS Statistics.

We propose a line of research that would complement existing models with a cloud prediction model (15-day forecasts are currently used) to provide both a short- and mid-term forecast that can be applied to predict global solar radiation that is closer to reality, at any time of year. Another possible line of research would be to generate a radiation model that minimises what is known as the "topographic effect" in satellite imagery classification, given that more than 99% of the information about the Earth's surface that is currently obtained comes from remote sensing and, more specifically, the capture of data from satellite-carried sensors.

References

- Bindi M, Gozzini B, 1998. Data spatial distribution in meteorology and climatology. Cost Action 79, Sept 28-Oct 3, 1997. Publ Office of the EU, Luxembourg. 226 pp.
- Changnon SA, Changnon D, 2005. Importance of sky conditions on the record 2004 Midwestern crop yields. *Phys Geogr* 26: 99-111. <https://doi.org/10.2747/0272-3646.26.2.99>
- Corripio JG, 2002. solarpath.zip. 18/09/2002. <http://tsunami.geo.ed.ac.uk/~jgc/.2002b>.
- Domínguez A, 2015. Modelado y análisis de parámetros agrometeorológicos para la optimización de la producción agrícola. Aplicación a las zonas regables de Extremadura. Doctoral thesis, Univ. de Extremadura, Badajoz, Spain.
- Estévez J, Gavilán P, Giráldez J.V, 2011. Guidelines on validation procedures for meteorological data from automatic weather stations. *J Hydrol* 402 (1-2): 144-154. <https://doi.org/10.1016/j.jhydrol.2011.02.031>
- Ferrante A, Mariani L, 2018. Agronomic management for enhancing plant tolerance to abiotic stresses: high and low values of temperature, light intensity and relative humidity. *Horticulturae* 4 (3): 21. <https://doi.org/10.3390/horticulturae4030021>
- Gattioni N, Boca T, Rebella C, Di Bella C, 2011. Comparación entre observaciones meteorológicas obtenidas de estaciones convencionales y automáticas a partir de la estimación de parámetros estadísticos. *Revista de Investigaciones Agropecuarias* 37: 75-85.
- Gozzini B, Hims S, 1998. Proceedings workshop dealing on spatialisation. Cost Action 79, Toulouse, 24-25 Sept 1996. Publ Office of the EU, Luxembourg. 149 pp.
- Gozzini B, Paniagua S, 2000. Coordination and comparison of several interpolation methods of meteorological data (minimum temperature). Cost Action 79: Integration of data and methods in agroclimatology. Publ Office of the EU, Luxembourg. 102 pp.
- Hantson S, Chuvieco E, 2011. Evaluation of different topographic correction methods for Landsat imagery. *Int J Appl Earth Observ Geoinform* 13 (5): 691-700. <https://doi.org/10.1016/j.jag.2011.05.001>
- Kambezidis HD, 2016. Current trends in solar radiation modeling: the paradigm of MRM. *J Fund Renew Energ Appl* 06 (2). <https://doi.org/10.4172/2090-4541.1000e106>
- Kaskaoutis D, Polo J, 2019. Editorial for the special issue "Solar Radiation, Modeling and Remote Sensing". *Remote Sens* 11 (10): 1198. <https://doi.org/10.3390/rs11101198>
- Lynch P, 2008. The origins of computer weather prediction and climate modeling. *J Comput Phys* 227 (7): 3431-3444. <https://doi.org/10.1016/j.jcp.2007.02.034>
- Matuszko D, 2012. Influence of the extent and genera of cloud cover on solar radiate n intensity. *Int J Climatol* 32: 2403-2414. <https://doi.org/10.1002/joc.2432>
- Michalakes J, Dudhia J, Gill D, Henderson T, Klemp J, Skamarock W, Wang W, 2004. The weather research and forecast model: software architecture and performance. Workshop on the Use of High Performance Computing in Meteorology, 25-29 Oct 2004, Reading UK. https://doi.org/10.1142/9789812701831_0012
- Mitjá A, Batalla E, 1982. Manual de radiación solar. Tablas para Catalunya. Universitat Politècnica de Catalunya i Instituto de Ciencias Energéticas -ETSIIB. Ed. Prensa XX1. Barcelona. 1: p. 137.
- Muneer T, Younes S, Munawwar S, 2007. Discourses on solar radiation modeling. *Renew Sust Energ Rev* 11 (4): 551-602. <https://doi.org/10.1016/j.rser.2005.05.006>
- Pandey CK, Kariyar AK, 2013. Solar radiation: models and measurement techniques. *Journal of Energy* 2013: Art ID 305207. <https://doi.org/10.1155/2013/305207>
- Pérez-Burgos A, Bilbao J, de Miguel A, Román R, 2014. Analysis of solar direct irradiance in Spain. *Energy Procedia* 57: 1070-1076. <https://doi.org/10.1016/j.egypro.2014.10.070>
- Polo J, Martín-Pomares L, Gueymard C.A, Balenzategui J.L, Fabero F, Silva JP, 2019. Fundamentals: quantities, definitions and units. In: *Solar resource mapping-fundamentals and applications; green energy and technology*; Polo J, Martín-Pomares L, Sanfilippo A, (Eds). Springer: Zurich, Switzerland. pp: 1-14. https://doi.org/10.1007/978-3-319-97484-2_1
- Psiloglou BE, Kambezidis HD, Kaskaoutis DG, Karagiannis D, Polo JM, 2019. Comparison between MRM simulations, CAMS and PVGIS databases with measured solar radiation components at the Methoni station, Greece. *Renew Energ* 146: 1372-1391. <https://doi.org/10.1016/j.renene.2019.07.064>
- Sandaña P, Ramírez M, Pinochet D, 2012. Radiation interception and radiation use efficiency of wheat and pea under different P availabilities. *Field Crops Res* 127: 44-50. <https://doi.org/10.1016/j.fcr.2011.11.005>

- Solanki SK, 2002. Solar variability and climate change: is there a link? *Astron Geophys* 43 (5): 9-13. <https://doi.org/10.1046/j.1468-4004.2002.43509.x>
- WMO, 1982. Observing the weather from space. World Meteorological Organization, Geneva. <https://public.wmo.int/en>
- Xiao S, Tian X, Liu Q, Wen J, Ma Y, Song ZA, 2018. A semi-empirical topographic correction model for multi-source satellite images. *ISPRS Ann Photogramm Remote Sens Spatial Inf Sci IV*: 225-232. <https://doi.org/10.5194/isprs-annals-IV-3-225-2018>
- Xue Y, Fennessy MJ, 1996. Impact of vegetation properties on U.S. summer weather prediction. *J Geophys Res* 101 (D3): 7419. <https://doi.org/10.1029/95JD02169>
- Zelenka A, Pérez R, Seals R, Remé D, 1999. Effective accuracy of satellite-derived hourly irradiances. *Theor Appl Climatol* 1 (62): 199-207. <https://doi.org/10.1007/s007040050084>
- Zhu X, Sun M, Wang Y, 2017. Correction of false topographic perception phenomenon based on topographic correction in satellite imagery. *IEEE Trans Geosci Remote Sens* 55 (1): 468-476. <https://doi.org/10.1109/TGRS.2016.2608980>
- Zimmermann NE, 2000a. Shortwavg.aml, 9.08.2000. http://www.wsl.ch/staff/niklaus.zimmermann/programs/aml1_1.html
- Zimmermann NE, 2000b. Diffuse.aml, 9.08.2000. http://www.wsl.ch/staff/niklaus.zimmermann/programs/aml1_4.html